THE EMERGING MAGNETIC FLUX AND THE ELEMENTARY ERUPTIVE PHENOMENON

Z. MOURADIAN, M. J. MARTRES, and I. SORU-ESCAUT

Observatoire de Paris – Meudon, LA 326, 92190 Meudon, France

(Received 27 November, 1981; in revised form 27 December, 1982)

Abstract. Observational studies before and during the flare start were made in Hα (3-λ heliograph at Meudon Observatory) on a large sample of 'elementary' flares, both on the disk and along the limb of the Sun. The concept of elementary eruptive phenomenon (EEP) is proposed to describe these observational data. The EEP may be considered as the basic element of complex flares which, then, are built up by the juxtaposition of several EEP. In the inferred scenario, the chromospheric eruptive phenomenon consists of two systems of loops: one cold – the surging arch – $T \simeq 10^4$ K, the other hot – the flaring arch –, covering a temperature range up to 10^7 K. The footpoints of the two systems remain differentiated until extinction of the phenomenon; their behaviour over time differs also. The surging arch (the magnetic flux emergence) rises first progressively in the solar atmosphere and the upper part of the loop is heated to coronal temperatures. The classical surge which is observed in the center of the Hα line, after the flash phase of the flare, is only the late development of the surging arch. The flaring arch originates from a pre-existing low loop, which is also able to rise in the solar atmosphere. These two systems coexist and may combine to form such physical characteristics as mass motion, expansion and post-flash phase.

1. Introduction

The overall goal of this study is to contribute to a better understanding of the relations existing between the different phases of flare build-up, starting from the concept of a simple flare. A new conceptual scenario, based on observations, is presented below. It differs from models proposed by certain other authors and reviewed by Canfield *et al.* (1980). Existing models generally leave some important problems unresolved, such as those formulated by Švestka (1981, p. 53): "We do not yet understand the relationship of flares to the various kind of mass ejecta (surges, sprays, eruptive prominences, coronal transients). In particular, active events on the limb often show characteristics that one can hardly reconcile with what we believe to know about flares from observations on the disk".

A variable wavelength heliograph, built by R. Michard, has been operating at the Observatoire de Meudon since 1966 (Banos, 1967). This instrument, functioning in continuous surveillance mode furnishes a set of three images per minute (Hα, Hα + 3/4 Å; Hα − 3/4 Å). It is thus adapted to the study of dynamic phenomena that precede and accompany flares. Such phenomena generally escape detection by non-automatic heliographs and by those instruments working only at Hα line center. The three adjacent bandwidths (0.75 Å) are obtained nearly simultaneously (within 15 s). Thus, we can observe without temporal and spectral discontinuities (over 2 Å), the start and the evolution of the movement of absorbant or emissive material in a given chromospheric structure. With this technique we have analysed more than a thousand flares.

Solar Physics **87** (1983) 309–328. 0038–0938/83/0872–0309$03.00.

From the analysed flares, we selected a sample of simple flares and we studied only their primary state of evolution, i.e. we neglected the expansion, the decreasing phase and the eventual post flare loops.

It is well known that flares are associated with Hα mass motions. These can be disturbances of preexisting filament* or transitory prominence like activity called 'active prominences' by Tandberg-Hanssen (1977, p. 97, 2b).

The dynamic, continuous process shown in this analysis, and the observational model derived from it, permit a better comparison between limb and disk observations of simple flares.

In Section 2 of the present paper we show the emergence of magnetic flux preceeding the flare start. In Section 3, the constitutive elements of the flare at its beginning are considered. In the last section and empirical model is suggested and discussed.

Preliminary results of this study have been submitted by Martres *et al.* (1981a, b).

2. The Surging Arch

2.1. Definition

The concept of flare (brightness, duration, surface) is essentially based on Hα brightening. Dynamic phenomena such as DB (Disparition Brusque), surge, etc. ..., are only associated with it and are considered as secondary. Observations of these phenomena, their frequency, and their importance over the entire Hα line profile suggest that they can play an important role in the mechanism of flare build-up. For example, Figures 1 and 2a show the evolution of two flares accompanied by movement of absorbant material. This Hα absorbing structure, which we call the '*surging arch*', appears first with a linear shape, lying near the flare site in the $B_{\|} = 0$ line (Figure 2b). Then, it evolves, rising archshaped without discontinuity when observed with our 3-λ technique. The archshaped development may be quite apparent as in Figure 1. Perspective effects play a very important role. However, we have noticed that in every case two components red and blue shifted simultaneous and not cospatial are present from the very beginning of the structure. The blue component is predominant at the beginning while the red one predominates during the final phase. They indicate the presence of material flowing along a magnetic loop while it emerges. Generally at the appearance of the flare (bright points), the shape of the surging arch changes drastically in Hα.

The observations performed with the 3-λ technique show that *the classical surge which is observed in the center of the Hα line after the flash phase of the flare is only the late development of the surging arch.*

Smith and Smith (1963, p. 107–109) relate earlier visual observations (1942–1951) of surge behaviour which are in good agreement with our analysis of the last phase of the surging arch.

* Note that we call 'filament' only the quiescent prominences and the relatively stable plage filaments (1 and 2a class of Tandberg-Hanssen, 1977, p. 97).

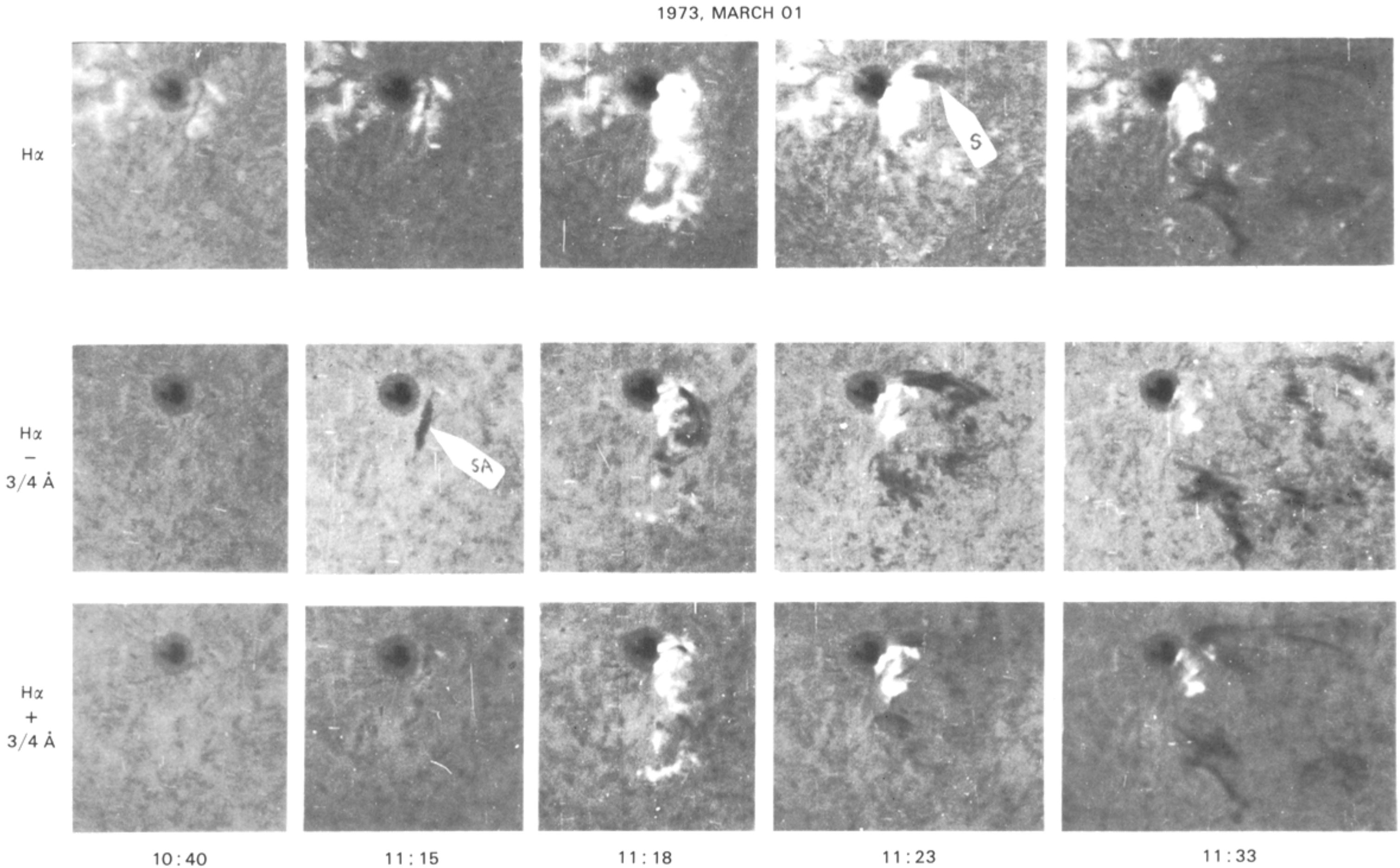

Fig. 1. Observation of the temporal evolution of a flare in Hα line center (top array) and in the wings. The arrows indicate the surge (S) and the surging arch (SA). This example shows that the surge is only the late and partial phase of the surging arch.

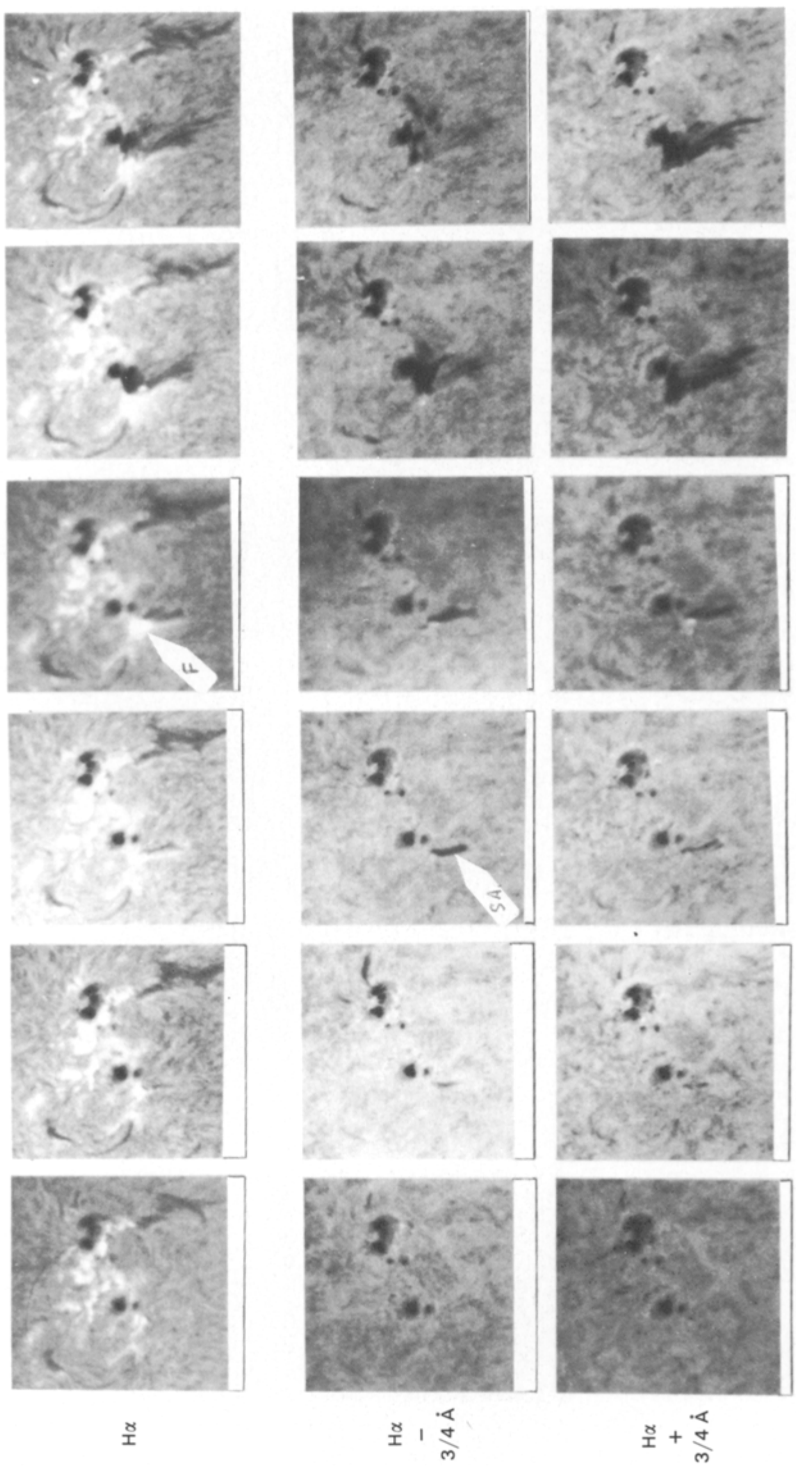

Fig. 2a. Temporal evolution of a surging arch and its associated flare. The arrows indicate the surging arch (SA) and the flare (F).

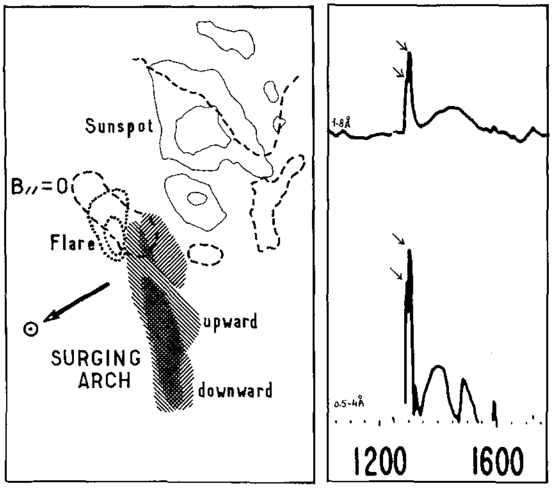

Fig. 2b. Same event as in Figure 2a. *Left*: Schematic drawing of the surging arch and the flare at 13 : 00 UT related to be $B_{\parallel} = 0$ lines (Meudon magnetogram at 13 : 29 UT). The main sunspot is at $\mu = 0.74$ and the direction of the disk center is also indicated. *Right*: The event in X-rays (GOES) is reported by the SGD. Note that the beginning of the burst is associated to the surging arch.

The following table describes the evolution of the complete phenomenon formed by the absorbant component (surging arch) and by the emissive component (flare):

Main phases	Figure 1	Figure 2a
No surging arch, no flare	10 : 40 UT	10 : 32 UT
Surging arch (mainly upward)	11 : 15 UT	12 : 30; 12 : 50 UT
Flare and surging arch	11 : 18 UT	13 : 00 UT
Decay of surging arch	11 : 23 UT	13 : 12 UT
Last phase of surging arch (mainly downward)	11 : 33 UT	13 : 16 UT
The expansion velocity of the surging arch in the sky plane	≥ 280 km s^{-1}	≥ 50 km s^{-1}

The velocities given above are in good agreement with those of the surges observed on the solar limb (Rust *et al.*, 1980, Table 7.1: 100 km s^{-1} and Banos and Dara-Papamargariti, 1983, 60–400 km s^{-1}). Note on the sketch in Figure 2b that the surging arch is rooted on the $B_{\parallel} = 0$ line, while the flare is anchored in both polarities.

2.2. Statistics

When a filament already exists at the flare site, its destabilization precedes the flare. The chromospheric dynamic preflare phenomena reviewed by Martin (1980), Van Hoven *et al.* (1980), and Hiei (1981) are of two types: activation of a preexisting filament or appearance of a preflare absorbing feature. To make statistical evaluation of the different classes of flares associated with these two types of instabilities we have taken material used by Martres *et al.* (1977). In that work, covering the period June 1970–September 1973, 81 flares listed in the *QBSA* (*Quarterly Bulletin on Solar Activity*) occured during patrol observations with the 3-λ heliograph. Of these 81 flares, eight were out of the field of the instrument: 73 flares remained for the statistical sample. In order to assure that the sample is representative we compare in Table I the distribution of the flares according to their importance to that given by Smith and Smith (1963, p. 64). We find good agreement between the obtained percentages and we conclude that our sample is unbiased and, thus that the results obtained are significant.

TABLE I

Comparative statistics of flare importance

	Smith and Smith (1963)	Present work
Total number	4699	73
	%	%
Subflare	75	71
Imp 1	20	25
Imp 2	5	4
Imp 3	0,5	0

(i) The observations used by Martres *et al.* (1977) are classed by us in the following categories:

– flare preceeded by activation of the filament	15 (26%)
– flares preceeded by a surging arch	34 (58%)
– flares without filament or surging arch	1 (2%) outside the spot 8 (14%) on the umbra.

(These categories are not linked to the importance of the flare). From our sample we excluded eight doubtful cases (difficult to precise if filament or surging arch) and seven cases situated too close to the limb.

In conclusion, more than half of the studied flares have not associated filament, but rather a surging arch visible in the wings of Hα which preceded the appearance of the flare; only a quarter of all cases can be associated with a destabilization of a filament.

(ii) For the studied sample we determined the delay between the beginning of the surging arch and the flare: the average is 11 min and the extreme values are 35 min and 1 min.

2.3. Discussion

In Axisa *et al.* (1973) some relationships between transitory Hα absorbing features prior to the flare (surging arches) and type III bursts were established. Kane *et al.* (1974) studied absorbing structures without flares and found that they are also associated with type III bursts and that some of them (7/15) have simultaneous soft X-ray emission. This means that type III radio bursts and soft X-ray emissions often accompany surging arches observed in the center and wings of Hα line, even in the absence of flare emission. Rust *et al.* (1977) found 6/54 cases in which X-ray emission might be associated with surge activity observed in the center of Hα line.

In Figure 2b we give an example of the X-ray burst (SGD–GOES) associated to the event given in Figure 2a. In both channels the beginning of the burst is associated with the surging arch at 12 : 50 UT. We note that this X-ray observation shows, as do many others a maximum which precedes the flare maximum (see arrows in Figure 2b).

2.4. Morphology of the surging arch

Among our Hα data we found two cases where a simultaneous EUV observation is available. In both, EUV emission is associated with a surging arch.

The June 16, 1973 event described below, includes surging arch and its flare (*Solar-Geophysical Data*: 18 : 11–18 : 33 UT).

The evolution of the complete phenomenon – surging arch and flare – is shown in Figures 3a and 3b and is described below:

A	1732	Appearance of a small and very weak brightness visible in Hα line center.
B	1745	Appearance of mainly upward flowing absorption material (surging arch) on $B_{\parallel} = 0$ (Figure 3a, arrow) and enhancement of 0–3 Å channel in SOLRAD-9 data (SGD).
	1750	Flow of absorption material in the form of a loop, upward in one leg and downward in the other.
	1753	Enhancement of the flare brightness and formation of an arch of absorbing material (surging arch).
C	1755	Surging arch in Hα continues.
C′	1755	No visible structure $T = 2 \times 10^6$ K in the Fe XVI line (from Eddy, 1979, p. 94) at the location of the surging arch.
	1803	Flash phase of the Hα emissive component. The anchor point of the surging arch situated out of the parasitic polarity is displaced.
D	1813	Surging arch and flare, the absorption is arch – shaped in Hα.
	1813–1827	(Figure 3b) Small bursts in hard and soft X-ray (lack of observations 1750–1812).
E	1818	Upper part of the surging arch disappears in Hα.
F	1822	Bright arch shape feature in the EUV (ATM Skylab, Reeves *et al.*, 1977) at the place of the upper part of the surging arch (Figure 3b).

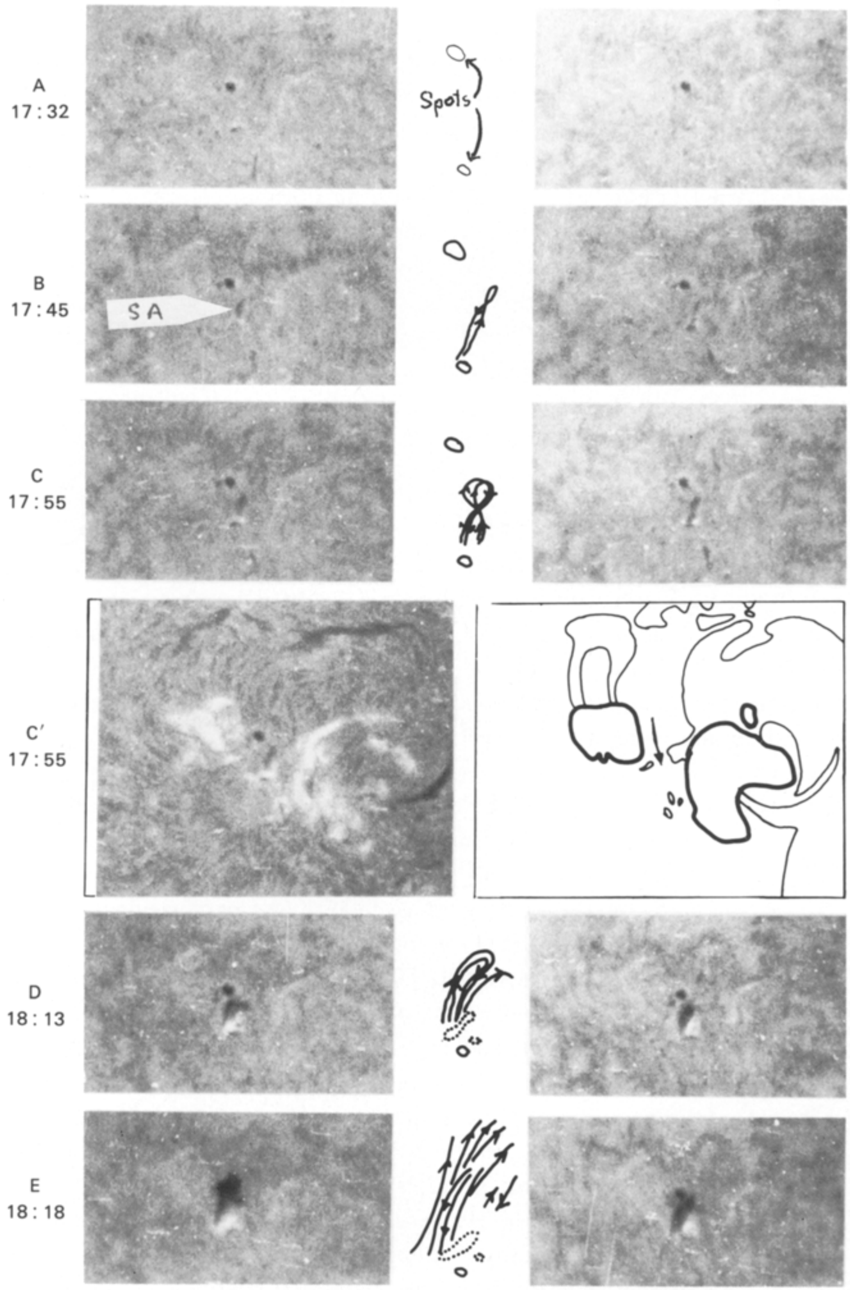

Fig. 3a. Development of the surging arch and the flare on June 16, 1973. For the five observations shown here (labelled A through E), the images in the wings of the Hα line (Hα − 3/4 Å, left; Hα + 3/4 Å, right) are given with the composite drawings which have been enlarged three times. The arrows represent movement of cold material, the dotted line Hα emission. At C′−1755 the Hα center line image is compared with the Fe XVI schema; note that at 2×10^6 K no structure is visible at the location of the surging arch (arrow).

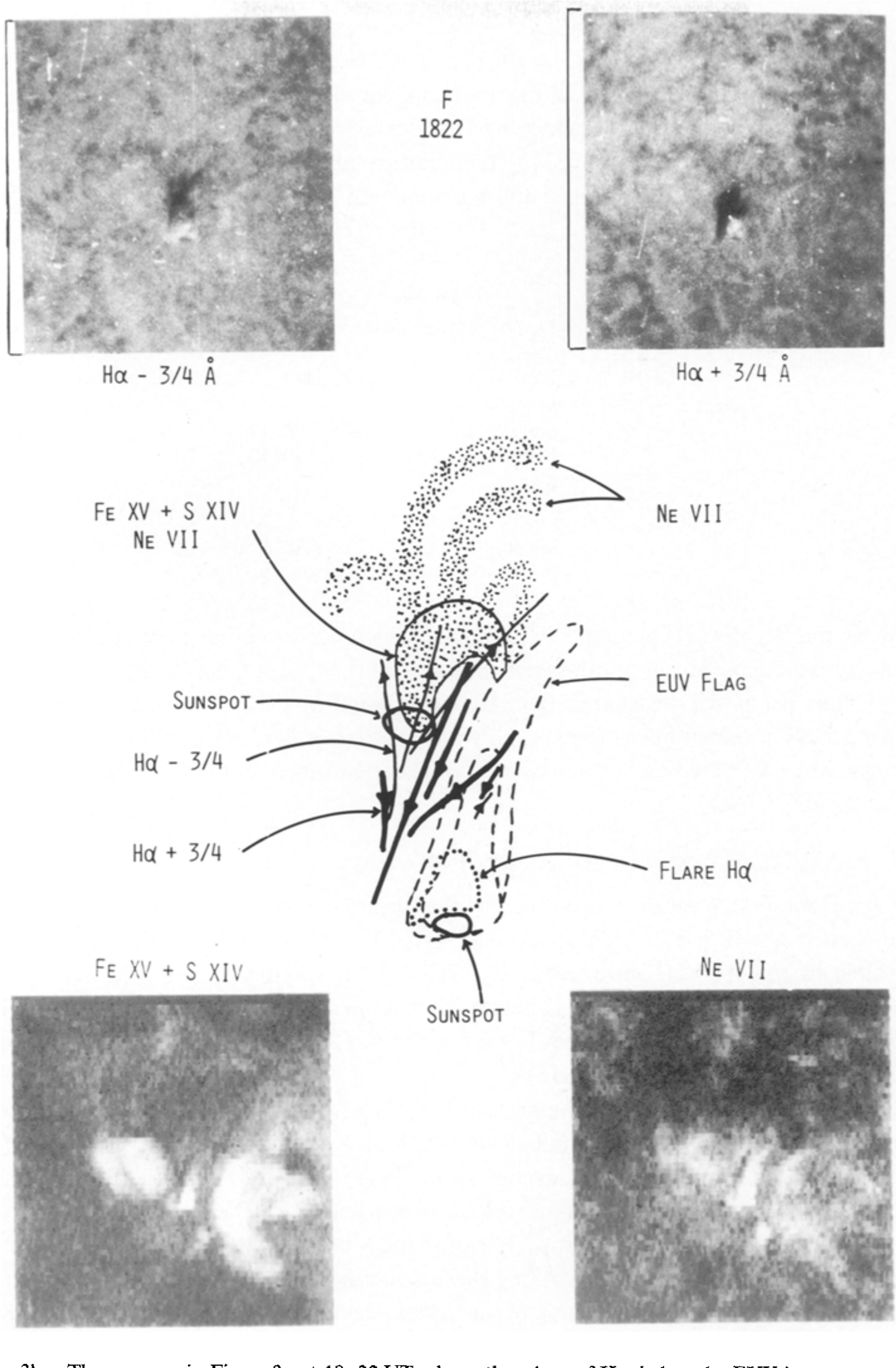

Fig. 3b. The same as in Figure 3a at 18 : 22 UT: above the wings of Hα; below the EUV images; center, composite drawing of these four images. The arrows represent movement of cold material, and the dotted hatching the EUV hot arch; these two systems form the surging arch. The 'flag' seen in EUV is shown with a broken line and the Hα flare with a dotted line.

No significant difference in shape appears in the observed temperature range (5×10^5 K $\leq T \leq 3 \times 10^6$ K). Concerning the flare, the Hα and EUV maxima coïncide. In Ne VII, Fe XV + S XIV, a 'flag-shaped' brightening is observed which shrouded this maximum. Table II gives the temperature range of the EUV data.

1832 Diminution of the phenomenon observed in Hα and end of the film.

TABLE II

HCO spectrometer detectors

Channel	Ion	T_{max}
3	Ne VII (465 Å)	4.8×10^5 K
4	Fe XV (417 Å)	2.5×10^6 K
	S XIV (417 Å)	
5	Fe XVI (335 Å)	2.0×10^6 K
	Mg VIII (335 Å)	2.3×10^5 K

Rust and Webb (1977) studied a major flare which occurred four hours before in the same active region but in another site. Figure 1 of their paper shows that during this major flare no activity existed in the flare site studied by us.

An event on September 1, 1980 is shown in Figure 4 of Martres *et al.* (1983): the Hα surging arch is outlined by S IV emission with an enhancement at the top (SMM–UVSP experiment).

2.5. Physical parameters of a surging arch

(i) *Temperature.* A surging arch is, at the beginning of its evolution, thermally homogeneous and at a low temperature ($T \sim 10^4$ K); it is entirely visible in Hα and is invisible in the EUV (Figure 3a, at C′ 1755). As a surging arch reaches altitudes $h \simeq 5 \times 10^4$ km its upper portion is heating, it disappears in Hα and becomes visible in the EUV, i.e., $T = 5 \times 10^5$ K and $T = 2.5 \times 10^6$ K (Figure 3b, at F 1822); the lower portions remain cool (visible in Hα).

Some authors have detected the presence of a hot structure (emitting in EUV) near flares, which shows that at the time of observations a hot feature existed (Kane *et al.*, 1974; Lites and Bruner, 1979; Doschek *et al.*, 1979; Hiei and Widing, 1979; Marsh *et al.*, 1981). All these observations are related to a structure which has the characteristics of our surging arch but the lack of Hα off-band observations prior to flare onsets prevented these authors from identifing these structures as surging arches. Webb and Jackson (1981) observed the heating of the top of a cool spray at the limb to $T > 10^5$ K.

(ii) *Density.* Hα photometry provides an estimate density of the surging arch. Since the legs have a geometry comparable to that of two spicules – two vertical cylinders – using the results of Beckers (1972), we obtain $N_e = 1$–3×10^{11} cm^{-3} and $T = 5 \times 10^4$ K at an approximate height $h = 3000$–4000 km.

The Ne VII spectroheliogram (Figure 3b) gives a rough value of the density at the top of the surging arch at June 16, 1980: $N_e = 10^{10}\ \text{cm}^{-3}$ at $T = 5 \times 10^5$ K. Hiei and Widing (1979) found for Fe XV, $N_e = 4 \times 10^{10}\ \text{cm}^{-3}$. Note that these two figures do not refer to the same event.

(iii) *Potential and kinetic energy.* The raising up to h_{max} of the material contained in a stretched loop (as we envision the surging arches) needs a potential energy of approximately

$$W_p(h_{\text{max}}) = 2 \int_0^{h_{\text{max}}} g(h)\,\rho(h)\,S(h)\,h\,\mathrm{d}h\,,$$

where g means the surface gravity, ρ the density, and S the section.

If we suppose that $g(h)$, $\rho(h)$, and $S(h)$ are constant with altitude (h), we obtain

$$W_p = g m_H N_e S h_{\text{max}}^2 .$$

For $N_e = 10^{10}\text{cm}^{-3}$, section $S = (10^4\ \text{km})^2$, and $h_{\text{max}} = 5 \times 10^4$ km, the potential energy is $W_p = 8 \times 10^{27}$ ergs. It is of the same order of magnitude as that of a very small chromospheric flare. Webb *et al.* (1980) mentioned energies of mass motions in flares of the order of 6–600 $\times\ 10^{27}$ erg. Hiei and Widing (1979) give for the potential energy of a structure which may be identified with a surging arch $W_p = 3 \times 10^{27}$ for $h_{\text{max}} = 2 \times 10^4$ km. The kinetic energy of the material of the June 16, 1973 surging arch with $v_{\text{H}\alpha} = 20\ \text{km s}^{-1}$ is

$$W_k = \tfrac{1}{2} m_H v^2 N_e V = 4 \times 10^{27}\ \text{erg}\,;$$

Hiei and Widing give $W_k = 6 \times 10^{27}$ erg.

Rust *et al.* (1980) give the physical characteristics for the cool part of the surging arch (surge) at $T = 8000$ K, $W_k = 5 \times 10^{27}$–5×10^{29} erg.

(iv) *Magnetic field.* Using photospheric magnetic field data, we compared the anchor points of the surging arch of Figure 2b with the line of inversion of polarity of the longitudinal field (Figure 2b). We interpret the surging arch as newly emerging magnetic flux in the chromosphere. It appeared first where the longitudinal field was nul, i.e., between two regions of opposite polarity independently of the μ position. Then, the anchor points span the $B_{\parallel} = 0$ line with a small angle. In the upper layers the loops of material can be used as tracers of lines of force.

We mention that Leroy (1982) measured the magnetic field of a surging arch at the limb and found ~ 40 G.

(v) *Velocity field.* Observations of surging arches show a flow on the order of $20\ \text{km s}^{-1}$. The direction of motion is always the same, rising along one branch and descending along the other. The motion continues even after the upper portion of the loop is heated (Figures 3a, b; Kane *et al.*, 1974; Lites and Brunner, 1979). This means that the magnetic loop is not yet broken and not yet reconnected.

In addition, the whole loop of a surging arch moves upward as shown in the table of Section 2.1.

2.6. About the 'Queens' Flare'

We have looked for structures which can be identified with the 'surging arch' in various papers describing the limb event of April 30, 1980.

De Jager *et al.* (1983) mentioned that during 18 min before the flare start, a loop filled with moving material was observed in EUV.

Woodgate *et al.* (1981) claimed that this flare was preceded by an arch visible in C IV which had "... a strong brightening at the foot point and the top of the loop as the main flare started".

In Rust *et al.* (1981), Figure 3 shows a preflare enhancement of the radio flux, 4 min before the flare start at 10.6 GHz.

Van Beek *et al.* (1981) observed near the flare a diffuse X component they called the 'tongue'.

These preflare structures seem to have the main characteristics of surging arch (cf. Figure 3 in Woodgate *et al.*, 1981).

3. The Flaring Arch

3.1. Elementary flares

There is general agreement among the authors (see review paper Michard, 1971) that in the chromosphere all the flares (even compact ones) appear to be formed of two distinct components situated on either side of a line of inversion of the magnetic field. The most extented eruptions, two-ribbon flares, generally appear when a (pre-existing) filament occupies the inversion corridor ($B_{\parallel} = 0$).

In all cases these flares reach their maximum extent from multiple points that appear locally well-separated and then merge to form the two components of the flare. This phenomenon has often been identified and cited (Michard *et al.*, 1964; Zirin, 1974). When there is a rapid start the multiple points appear nearly simultaneously ($\Delta t < 1$ min). With a slower start, the expansion is better observed. Figure 4 shows two examples of great flares. At line center the flare appears as a non-structured mass but in the wings of the line the different pairs of starting points can be clearly distinguished. This means that we may hypothesize that they are the constitutive elements of large flares – and call them '*elementary flares*'.

This concept is not to be confused with the elementary flare bursts observed by Van Beek *et al.* (1974) and by De Jager and De Jonge (1978) which are fine structures seen in hard X-ray emission (~ 1 s). Events of this time scale are beyond the range of our instrument which has a temporal resolution of one minute.

3.2. Spatial morphology

We will follow the first instants of development of the spatial form of a flare near the limb anchored on bright points on the disk; the flare of August 11, 1972, is shown in

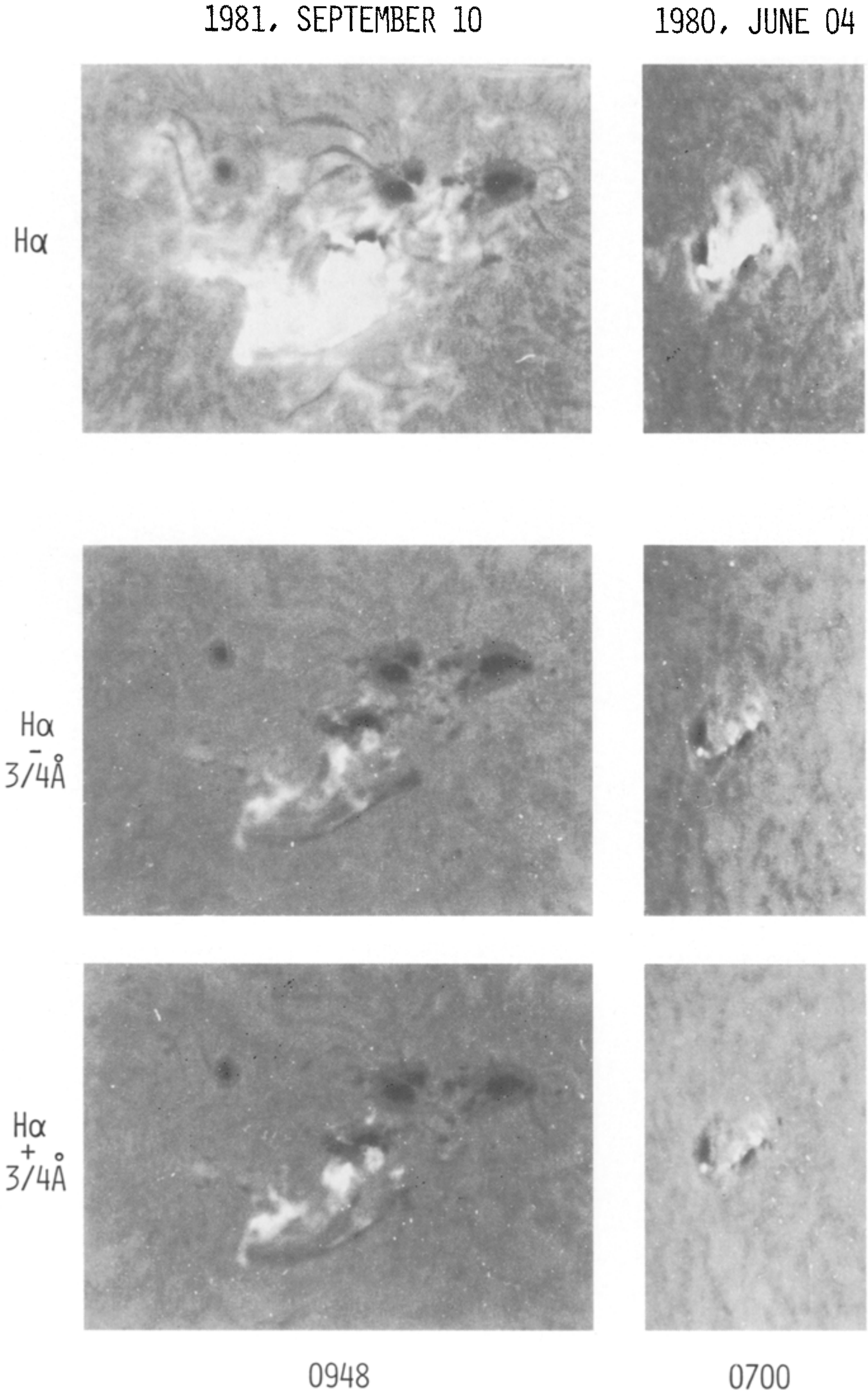

Fig. 4. Examples of complex flares at Hα line center (first array). Note the individual points visible in the wings of the Hα line.

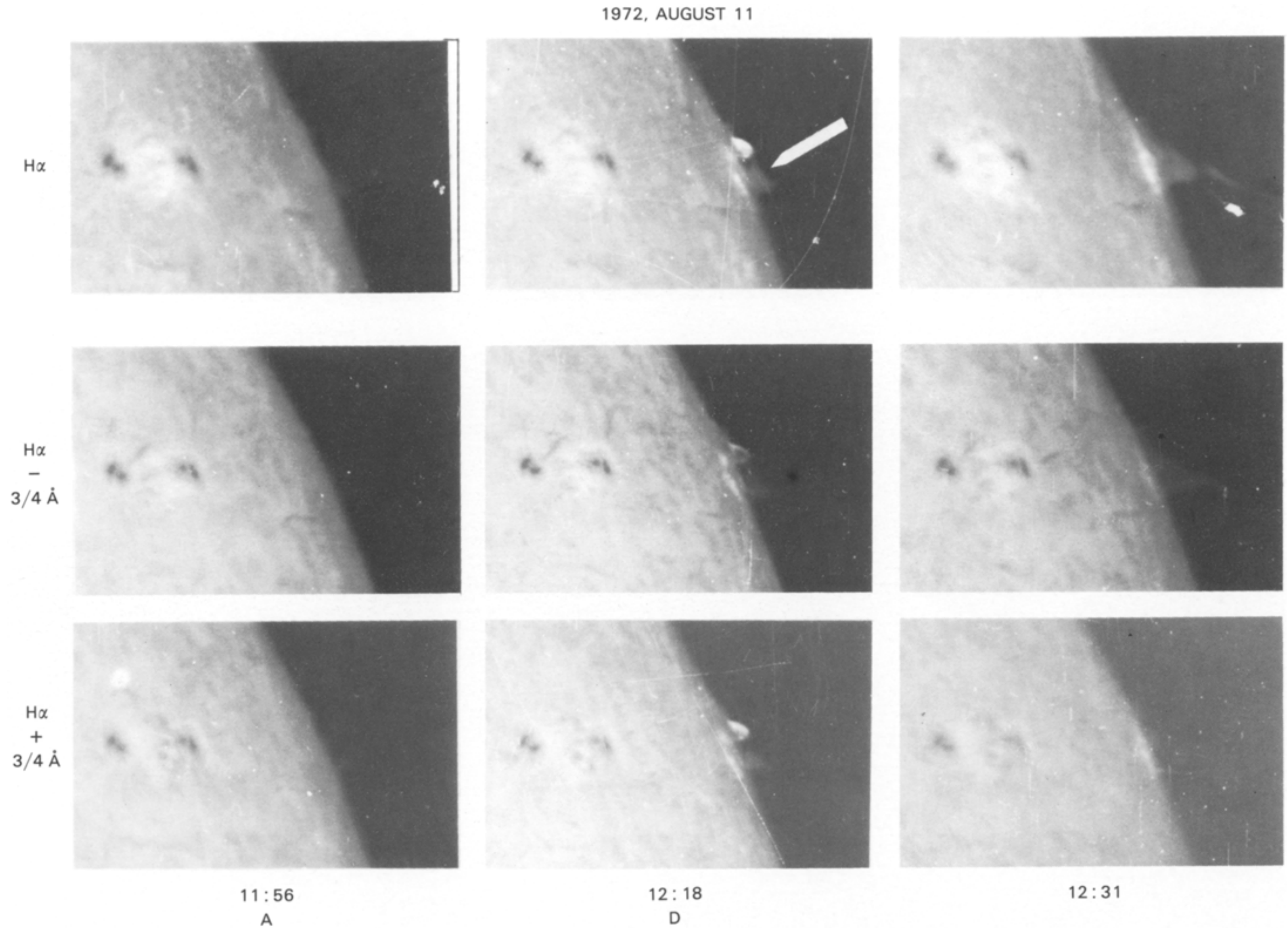

Fig. 5. Development of a simple flare on the limb, 1972, August 11. The letters indicate approximately the same moments of the evolution as those of Figures 3a and 3b. The arrow indicates the surging arch.

Figure 5:

1212 Appearance of a surging arch with vertical motion (not shown).

1217 Development in altitude of the surging arch feature and first appearance of the bright points (not shown).

D 1218 Strong emission of the flare in the shape of a loop ($h \simeq 10\,000$ km). It rises first from one of the bright points and becomes progressively brighter as it rises, curving towards the second bright point which, itself rises slightly. The loop does not appear to close completely on itself. Throughout the evolution, the loop and the feet rest approximately in the same plane, perpendicular to the magnetic inversion line. The rising branch seems much larger than the other. We call this structure a *flaring arch*; the pair of bright points visible on the disk are its anchorage points.

1220 End of flaring arch (not shown).

1231 Only the surging arch is visible.

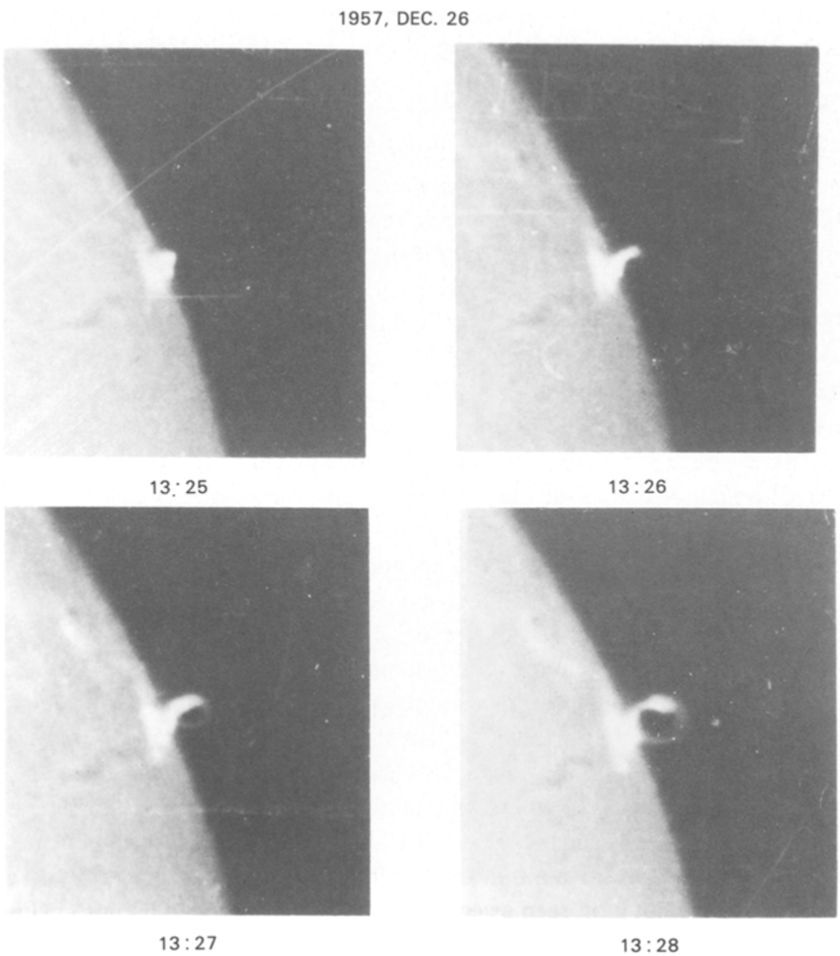

Fig. 6. The flare on December 26, 1957: another type of flaring arch on the limb.

This observation has been reported, in extenso, by Martres (1973). Among the examples reported by Smith and Smith (1963, p. 87) and by Moriyama (1977), to which we may add the observations made at the Meudon Observatory, two types of flaring arches may be identified:

(a) as illustrated by the observation at 12:18 in Figure 5, mentioned above, and

(b) as illustrated in Figure 6 in which the process of evolution is the same (with differences between the two branches), but the loop does not remain in the same plane as its feet; it seems to be subjected to a spiral movement.

In both cases, observations show that the flaring arch appears first to be very low and nearly circular. Rust *et al.* (1981) in the Hα description of the April 30, 1980 flare pointed out that the flaring loop had a height of about 3500 km. In the case of June 16, Figure 3, the brightening of the flaring arch increased preferentially from the parasitic polarity.

At the expansion phase, when it exists, a flaring arch suffers a sudden perturbation, it breaks up and the flare rises up. In this phase, reconnections may take place.

We think that the flag-shaped feature observed at 18:22 on June 16, 1973 in EUV as shown in Section 2.4, is a EUV structure superimposed on the flaring arch (Figure 3b).

3.3. Physical Parameters of Flaring Arches

(i) *Temperature.* The flaring arch has, from the moment of its appearance, a high temperature and is thermally inhomogeneous. This feature can be observed in Hα, in EUV, in soft X-rays, implying a very large range of temperature from 10^4 to 10^7 K as observed by Gabriel *et al.* (1981) for the Queen's flare which seems to belong also to the simple flare class.

(ii) *Magnetic field.* The flaring arch outlines the magnetic field. As seen above, on limb observations, it appears as a loop, at the beginning. On disk observations, the two bright points appear simultaneously on each side of a $B_{\parallel} = 0$ line. This means that the Hα flare affects a pre-existing magnetic loop.

If the flare were the emergence of magnetic field, it would appear on the disk as a single elongated bright structure at the beginning and only later would it become a two-component feature. The observations never agree with this scenario.

On the other hand, we note that the anchor points of the hot loop and the surging arch are never in the same place: the axis of the anchorage points of the flaring arch is generally quasi-perpendicular to the $B_{\parallel} = 0$ line direction. It is a very different situation from that of the surging arch (see above).

Figure 7 indicates the apparent positions of the anchor points of the surging and flaring arches. Their displacements (5–7 km s^{-1}) measured over time are schematized.

Seen on the disk, the flaring arch, at its beginning, shows no radial velocities higher than 5 km s^{-1}. Some measurements with another technique give, for the rising velocity, a value of 2–3 km s^{-1} (Mein and Mein, 1981). However, for flares observed on the limb (Moriyama, 1977; Figure 13 in Smith and Smith, 1963; Meudon heliograph) the upward velocities along the hot loop seen as emission in Hα, can reach 200 km s^{-1} (Figure 6). Thus, the measurements of the component of the velocity perpendicular to the surface of the Sun are not concordant with the disk observations. The measurements made on

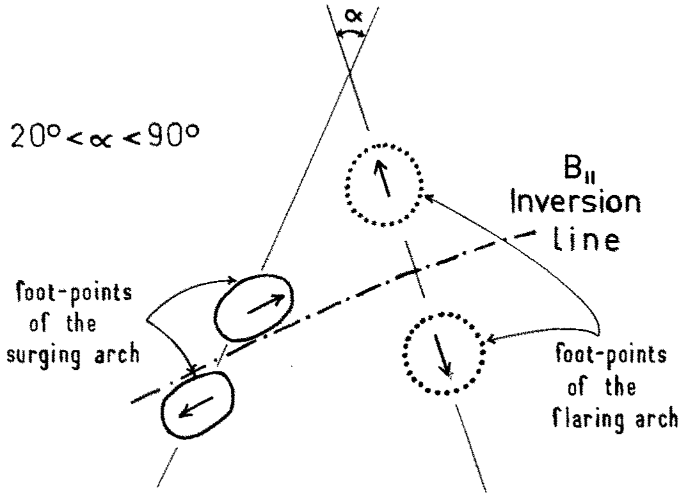

Fig. 7. Schematic relative positions of foot points of a surging arch (full line) and the associated flaring arch (dotted line). Note that the foot points are not cospatial. The arrows indicate their displacements observed over time.

the disk show Doppler effects, hence, mass motions. The velocity observed on the limb must be then the propagation of the excitation of the Hα line in a magnetic field loop filled with pre-existing material that cannot be observed in Hα before the flare start.

After the formation of the hot arch, it can either keep its initial shape while reducing intensity (static flare – Figures 2 and 3), or expand towards the corona with mass motions (dynamic flare – Figures 1 and 4). In this case the Hα material may expand and gain altitude with a velocity of about 100 km s^{-1}.

4. Elementary Eruptive Phenomenon (EEP) – Observed Scenario

In the present work we studied the simple flare (flaring arch) and its associated surging arch. The two components seem to have independant temporal evolution. Together they form that we call the 'elementary eruptive phenomenon' (EEP).

As shown in Section 2.5 (iii) the potential and kinetic energy of the surging arch is of the same order of that of the flaring arch, so we conclude that the behaviour of the two structures must be taken in account into the energy budget of the EEP and more generally of the flares.

Below we give the observational scenario of the first phase of an EEP based on the study of several EEP-s.

The surging arch begins several minutes before the start of the flare and lasts as long as the flare itself and often longer. The magnetic field of the surging arch is on the order of 40 G (Section 2.5 (iv)); the density $\sim 10^{11}$ cm^{-3} and the temperature $\sim 10^4$ K. This arch can have a twisted shape. The material in the interior of the loop has a velocity on the order of 20 km s^{-1} and the ascending velocity of the whole loop is > 50 km s^{-1} and can reach 400 km s^{-1}. The top of this arch heats up, reaching temperatures of 10^5–10^6 K. Sometimes it is accompanied by type III and X-ray bursts (Section 2.3).

The flaring arch or 'flare' appears in a pre-existing magnetic loop, low and circular shaped. It is composed of dense and hot (10^4–10^7 K) material. Velocities in the interior of the hot loop seem to be low. Note that the anchor points of the hot loop and the surging arch are never in the same place (Figure 7).

5. Remarks

(i) In flares associated with the destabilization of a pre-existing filament, the destabilization may be due to the emergence of a surging arch located below it. Some recent observations of emergence of a new magnetic flux close to filaments seem in good agreement with this statement (Martin *et al.*, 1983; Gaizauskas, 1983).

(ii) The magnetic field of the two loops rising towards the corona may collide with the pre-existing field of the active region. The reconnection of the lines of force does not appear to be the basic trigger mechanism but, as a possible consequence of the flare.

(iii) Because the top of the surging arch is heated (Machado and Emslie, 1979) and reaches coronal temperature just before, or at the same time, as the start of the flaring arch, we think that it is precisely this structure which led to the idea that the flare is triggered in the corona. More intensive study of complete eruptive phenomena should be made with appropriate coordinated observations in X, EUV, optical and radio wavelengths.

We must not that the surging arch has a poor probability to be observed on the disk with a filter working in the center of the Hα line. When the structures, located on the disk, have the same velocities as those measured on the limb (50–400 km s^{-1}) they are outside the bandwidth. For instance, structures having velocities > 30 km s^{-1} pass undetected with a 0.5 Å bandwidth on Hα.

We hope that the concept of EEP will aid the reconciliation of center and limb observations of flares. Further study of the interactions of neighbouring EEP-s will provide a better understanding of extended flares.

Acknowledgements

The authors are very grateful to Dr D. M. Rust for his helpful comments and his critical reading of the manuscript. Dr R. W. Noyes provided EUV data from the ATM experiment aboard Skylab and Dr B. Woodgate, SMM data. One magnetogram is due to the courtesy of Prof. H. Zirin and another one to Dr J. Rayrole.

They thank G. Servajean and J. R. Frémy for preparing the photographic material, G. Prieur for typewriting.

References

Axisa, F., Martres, M. J., Pick, M., and Soru-Escaut, I.: 1973, *Solar Phys.* **23**, 159.
Banos, G.: 1967, *Solar Phys.* **1**, 397.
Banos, G. and Dara-Papamargariti, H.: 1983, *Astron. Astrophys.* **120**, 181.
Beckers, J. M.: 1972, *Ann. Rev. Astron. Astrophys.* **10**, 73.

Canfield, R. C., Brown, J. C., Brueckner, G. E., Cook, J. W., Craig, I. J. D., Doschek, G. A., Emslie, A. G., Henoux, J.-C., Lites, B. W., Machado, M. E., and Underwood, J. H.: 1980, in P. A. Sturrock (ed.), *Solar Flares*, Colorado Assoc. Univ. Press, p. 231.
Doschek, G. A., Feldman, U., and Mason, H. E.: 1979, *Astron. Astrophys.* **73**, 74.
Eddy, J. (ed.): 1979, *The New Sun*, NASA SP-402.
Gabriel, A. H., Acton, L. W., Culhane, J. L., Philips, K. J. H., Wolfson, C. J., Rapley, C. G., Antonucci, E., Bentley, R. D., Jordan, C., Kayat, M. A., Leibacher, J. W., Levay, M., Sherman, J. C., Strong, K. T., and Veck, N. J.: 1981, *Astrophys. J.* **244**, L147.
Gaizauskas, V.: 1983, in Z. Švestka, D. M. Rust, and M. Dryer (eds.), *XXIV COSPAR, Symp. Solar Maximum Year*, Ottawa, Advances in Space Research, Pergamon Press, p. 11.
Hiei, E.: 1981, in F. Moriyama and J. C. Henoux (eds.), *Proceedings of the Japan–France Seminar on Solar Physics*, p. 185.
Hiei, E. and Widing, K. G.: 1979, *Solar Phys.* **61**, 407.
De Jager, C. and De Jonge, G.: 1978, *Solar Phys.* **58**, 127.
De Jager, C., Machado, M., Schadee, A., Strong, K., Švestka, Z., Woodgate, B. E., and Van Tend, W.: 1983, *Solar Phys.* **84**, 205.
Kane, S. R., Kreplin, R. W., Martres, M. J., Pick, M., and Soru-Escaut, I.: 1974, *Solar Phys.* **38**, 483.
Leroy, J. L.: 1982, private communication.
Lites, B. E. and Bruner, E. C.: 1979, *Astrophys. J.* **228**, 322.
Machado, M. and Emslie, G. A.: 1979, *Astrophys. J.* **232**, 903.
Marsh, K. A., Hurford, G. J., Zirin, H., Dulk, G. A., Dennis, B. R., Frost, K. J., and Orwig, L. E.: 1981, BBSO Preprint No. 200.
Martin, S.: 1980, *Solar Phys.* **68**, 217.
Martin, S., Deszö, L., Antalová, A., Kučera, A., and Harvey, K. L.: 1983, in Z. Švestka, D. M. Rust, and M. Dryer (eds.), *XXIV COSPAR, Symp. Solar Maximum Year*, Ottawa, Advances in Space Research, Pergamon Press, p. 39.
Martres, M. J.: 1973, *WDCA for Solar Terrestrial Physics Report 28*, Part I, p. 52.
Martres, M. J., Soru-Escaut, I., and Nakagawa, Y.: 1977, *Astron. Astrophys.* **59**, 255.
Martres, M. J., Mouradian, Z., and Soru-Escaut, I.: 1981a, in F. Moriyama and J. C. Henoux (eds.), *Proceedings of the Japan–France Seminar on Solar Physics*, p. 188.
Martres, M. J., Mouradian, Z., and Soru-Escaut, I.: 1981b, *Congrès de la Société Française de Physique*, p. 257.
Martres, M. J., Mein, N., Mein, P., Mouradian, Z., Rayrole, J., Schmieder, B., Simon, G., Soru-Escaut, I., Strong, K., and Woodgate, B.: 1983, in Z. Švestka, D. M. Rust, and M. Dryer (eds.), *XXIV COSPAR, Symp. Solar Maximum Year*, Ottawa, Advances in Space Research, Pergamon Press, p. 109.
Mein, N. and Mein, P.: 1981, private communication.
Michard, R.: 1971, in R. Howard (ed.), 'Solar Magnetic Fields', *IAU Symp.* **43**, 359.
Michard, R., Mouradian, Z., Olivieri, G., and Soru-Escaut, I.: 1964, *Notes et inf. Obs. de Paris* **XX**, *Astrophys.* 5.
Moriyama, F.: 1977, *IQSY Report on Solar Phenomenon in 1972–1974*, p. 7.
Reeves, E. M., Hubert, M. C. E., and Timothy, J. G.: 1977, *Apl. Opt.* **16**, 837.
Rust, D. M. and Webb, D. F.: 1977, *Solar Phys.* **54**, 403.
Rust, D. M., Webb, D. F., and Maccombie, W.: 1977, *Solar Phys.* **54**, 53.
Rust, D. M., Hildner, E., Dryer, M., Hansen, R. T., Mc. Clymont, A. N., McKenna-Lawlor, S. M. P., McLean, D. J., Schmahl, E. J., Steinolfson, R. S., Tandberg-Hanssen, E., Tousey, R., Webb, D. F., and Wu, S. T.: 1980, in P. A. Sturrock (ed.), *Solar Flares*, Colorado Assoc. Univ. Press, p. 274.
Rust, D. M., Benz, A., Hurford, G. J., Nelson, G., Pick, M., and Ruždjak, V.: 1981, *Astrophys. J.* **244**, L179.
Smith, H. J. and Smith, E. v. P.: 1963, *Solar Flares*, McMillan Co., New York.
Švestka, Z.: 1981, in E. R. Priest (ed.), *Solar Flare Magnetohydrodynamics*, Gordon and Breach Sci. Publ., p. 53.
Tandberg-Hanssen, E.: 1977, in A. Bruzek and C. J. Durrant (eds.), *Illustrated Glossary for Solar and Solar Terrestrial Physics*, D. Reidel Publ. Co., Dordrecht, Holland, p. 106.
Van Beek, H. F., de Feiter, L. D., and De Jager, C.: 1974, *Space Res.* **XIV**, 447.
Van Beek, H. F., de Jager, C., Fryer, R., Schadee, A., Švestka, Z., Boelee, A., Duijveman, A., Galama, M., Hoekstra, R., Hoyng, P., Imhof, J. R., Lafleur, H., Machado, M. E., Maseland, H. V. A. M., Mels, W. A., Schrijver, J., Simnett, G. M., Van der Laan, J. J. M., Van Rens, P., Van Tend, W., Werkhoven, F., Willmore, A. P., Wilson, J. W. G., and Zandee, W.: 1981, *Astrophys. J.* **244**, L157.

Van Hoven, G., Anzer, U., Barbosa, D. D., Birn, J., Cheng, C. C., Hansen, R. T., Jackson, B. V., Martin, S. F., McIntosh, P. S., Nakagawa, Y., Priest, E. R., Reeves, E. M., Reichmann, E. J., Schmahl, E. J., Smith, J. B., Solodyna, C. V., Thomas, R. J., Uchida, Y., and Walker, A. B. C.: 1980, in P. A. Sturrock (ed.), *Solar Flares*, Colorado Assoc. Univ. Press, p. 17.

Webb, D. F. and Jackson, B. V.: 1981, *Solar Pjhys.* **73**, 341.

Webb, D. F., Cheng, C. C., Dulk, G. A., Edberg, S. J., Martin, S. F., McKenna-Lawlor, S., and McLean, D. J.: 1980, in P. A. Sturrock (ed.), *Solar Flares*, Colorado Assoc. Univ. Press, p. 471.

Woodgate, B. E., Shine, R. A., Brandt, J. C., Chapman, R. D., Michalitsianos, A. G., Kenny, P. J., Bruner, E. C., Rehse, R. A., Schoolman, S. A., Cheng, C. C., Tandberg-Hanssen, E., Athay, R. G., Beckers, J. M., Gurman, J. B., Henze, W., and Hyder, C. L.: 1981, *Astrophys. J.* **244**, L133.

Zirin, H.: 1974, in A. Beer (ed.), *Vistas Astron.* **16**, 1.